THE JOURNAL OF PHYSICAL CHEMISTRY Letters

Letter

pubs.acs.org/JPCL

Freezing of Molecular Motions Probed by Cryogenic Magic Angle Spinning NMR

Maria Concistrè,[†] Elisa Carignani,[‡] Silvia Borsacchi,[‡] Ole G. Johannessen,[†] Benedetta Mennucci,[‡] Yifeng Yang,[§] Marco Geppi,[‡] and Malcolm H. Levitt*[,†]

[†]School of Chemistry, University of Southampton, SO17 1BJ Southampton, United Kingdom

[‡]Dipartimento di Chimica e Chimica Industriale, Università di Pisa, Via Risorgimento 35, 56126 Pisa, Italy

[§]School of Engineering Science, University of Southampton, Southampton, United Kingdom

S *Supporting Information*

ABSTRACT: Cryogenic magic angle spinning makes it possible to obtain the NMR spectra of solids at temperatures low enough to freeze out most molecular motions. We have applied cryogenic magic angle spinning NMR to a crystalline small-molecule solid (ibuprofen sodium salt), which displays a variety of molecular dynamics. Magic angle ^{13}C NMR spectra are shown for a wide range of temperatures, including in the cryogenic regime down to 20 K. The hydrophobic and hydrophilic regions of the molecular structure display different behavior in the cryogenic regime, with the hydrophilic region remaining well-structured, while the hydrophobic region exhibits a broad frozen conformational distribution.

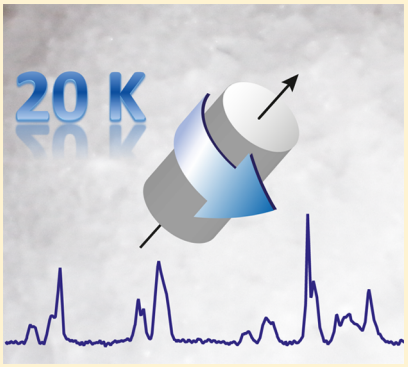

SECTION: Spectroscopy, Photochemistry, and Excited States

Magic angle spinning (MAS) NMR is an essential tool in the study of solid-state materials. The rapid rotation of the sample about the "magic angle" (arctan $(2)^{1/2} \cong 54.7°$) with respect to the main magnetic field averages out anisotropic nuclear spin interactions and leads to improved spectral resolution and sensitivity. Recent technical advances have made it possible to perform MAS NMR in the cryogenic temperature regime.[1−7] There are several motivations for low-temperature MAS NMR; NMR signals are stronger at low temperatures due to Curie law nuclear paramagnetism, the radio frequency noise in the receiver coil is reduced at the same time, the study of cryogenic solid-state phenomena such as superconductivity[8] and quantum molecular rotation[9] become possible, and in the context of biomolecular NMR, low-temperature operation makes it possible to trap and study intermediate and functional states of proteins.[10−13] Furthermore, the combination of MAS NMR with dynamic nuclear polarization (DNP) provides large NMR signal enhancements at low sample temperatures, which is particularly important for biomolecular structural studies.[14−23]

Typically, molecular motions influence the NMR spectra of solids in a temperature-dependent fashion.[24−28] Three temperature regimes are relevant. At high temperature, where the molecular motion is more rapid than the time scale of nuclear spin interactions, the molecular motion leads to line narrowing, through the averaging of inhomogeneous interactions. Reduction of temperature slows the motion and may bring the nuclear spin system into the intermediate exchange regime, in which the time scales of the motion and of the nuclear spin interactions are similar; this typically leads to strong line broadening. At still lower temperatures, the molecular motions are slowed down further or frozen. This may lead to either a narrowing of the spectrum as the motion becomes too slow to influence the spectral line widths (LWs) or, in some cases, a persistence of endemic spectral broadening because a wide range of molecular conformations are frozen in, each with different spin interaction parameters such as chemical shifts. It is interesting to explore the conditions under which very low sample temperatures lead to broadening, or narrowing, of the solid-state NMR spectra.

Commercial NMR equipment cannot normally access temperatures low enough to enter the slow or frozen-motion regime for the full range of molecular motions in a solid. The development of equipment capable of performing stable MAS NMR on samples at temperatures below 25 K has now made it possible to investigate this issue.[1−4] The equipment used in this work is available at the University of Southampton (U.K.) and allows MAS experiments to be run at a temperature as low as 9.6 K.[9]

This report applies to the case of sodium ibuprofen dihydrate, (sodium (*RS*)-2-(4-(2-methylpropyl)phenyl)-propanoate dihydrate, molecular formula $Na^+ C_{13}H_{17}O_2^- \cdot$

Received: December 3, 2013
Accepted: January 15, 2014
Published: January 15, 2014

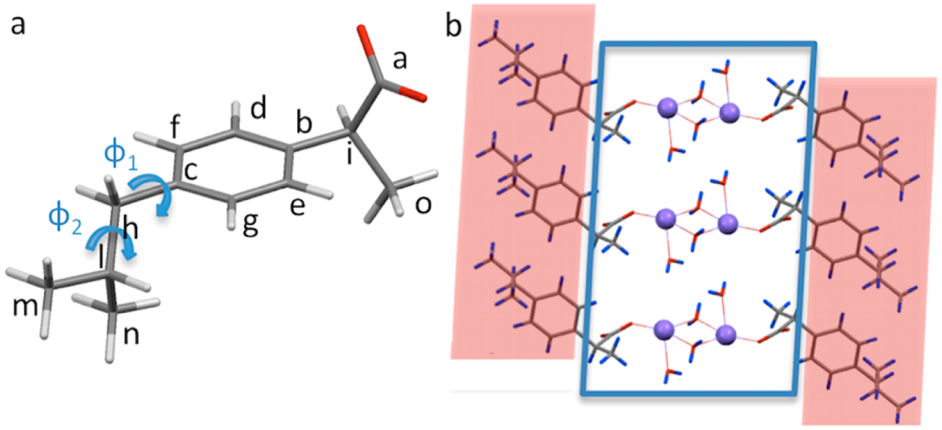

Figure 1. (a) Chemical structure of the ibuprofen anion showing the labeling of the ^{13}C sites and the torsional angles of the isobutyl moiety. (b) Crystal structure of IBU-S (CCDC number 285650).[30] Sodium atoms are indicated by purple spheres coordinated by ibuprofen anions and water molecules. The red and blue rectangles indicate the hydrophobic and hydrophilic regions, respectively.

$2H_2O$), referred to here as IBU-S; see Figure 1. This compound presents a relatively simple ^{13}C NMR spectrum in the solid state and an interesting dynamic behavior, with different fragments characterized by motions on the nanosecond time scale at room temperature. Its internal molecular motions have already been characterized at a conventional range of temperatures by solid-state NMR.[29] Furthermore, the crystal structure[30] of IBU-S presents two classes of molecular environment. The charged carboxylate groups, the sodium ions, and the associated waters of hydration form a hydrophilic plane in the crystal structure. The hydrophobic isobutyl groups are organized in separate, parallel planes (Figure 1).

The aim of this Letter is the study of dynamical processes occurring in IBU-S in the cryogenic regime. We describe cryogenic MAS NMR experiments, with particular attention on the dependence of ^{13}C LWs on temperature. As mentioned above, two scenarios are possible when the sample is cooled into the cryogenic temperature regime: (1) Cryogenic line narrowing: If the system settles into a single, minimum-energy conformation, the NMR peaks become narrower as the sample gets colder, and the molecular motion becomes too slow to broaden the peaks. (2) Cryogenic line broadening: If the molecular motion explores a large number of conformations, each at a local minimum of a highly corrugated potential energy surface, the NMR spectrum is expected to display considerable inhomogeneous broadening in the cryogenic regime because a large number of inequivalent conformations are "frozen in", each displaying different chemical shifts.

^1H-decoupled ^{13}C-CP-MAS spectra of IBU-S were recorded on four different sets of NMR apparatus at temperatures ranging from 358 to 20 K (Figure 2). The experimental details, including rotor diameters, spinning frequencies, magnetic field strengths, rf field strengths, and details of the cryogenic MAS equipment, are given in the Supporting Information (SI). The peak assignments for the high-temperature spectra are taken from ref 31.

The behavior of the ^{13}C-CP-MAS spectra of IBU-S at temperatures above ~223 K has been described previously.[29] The main feature is the broadening of the ^{13}C peaks from the aromatic sites (**d**,**e**,**f**,**g**) as the temperature is reduced. This behavior is attributed to 180° flips of the aromatic ring, which pass into the intermediate exchange regime at around ~260 K. Cooling below this temperature takes the ring flips into slow exchange. In the range of 139−185 K, the complex spectral region at around 128 ppm may be interpreted in terms of one peak at 128.4 ppm and three overlapping signals centered at 130.6, 129.8, and 128.9 ppm. These four resonances are associated with the distinct aromatic sites **d**, **e**, **f**, and **g**. The presence of all four peaks expected for the carbons **d**−**g** indicates that the frequency of the π-flip is lower than 100−200 Hz below 195 K. Additionally, below 195 K, the aromatic ring seems to be frozen in a single conformation, and the broadening observed at a temperature lower than 139 K is partially due to the superimposition with a spinning side band of the carboxylic carbon signal.

A similar phenomenon occurs for the isobutyl resonances (**h**, **l**, **m**, **n**) but at lower temperature. All of these resonances are sharp (LW at half-height ≈ 1.5 −2.0 ppm) at high temperature but become broad below ~160 K due to intermediate-regime conformational exchange of the isobutyl moiety, reaching a maximum broadening at around 120 K. The ^{13}C peak of the methyl site **o** also broadens strongly at ~160 K, which is attributed to intermediate-regime-hindered rotation of the methyl group about the ternary axis.

The cryogenic regime below 120 K is the main focus of attention in this Letter. The peaks associated with ^{13}C sites in the *hydrophilic* region of the crystal structure (**a** and **i**) remain relatively sharp (LW at half-height ≈ 2.0 ppm) in the cryogenic regime. Furthermore, the methyl peak **o**, which is also associated with the hydrophilic region of the structure, is so broad as to be invisible at ~120 K due to intermediate-regime three-fold rotation but sharpens considerably (LW at half-height ≈ 4.0 ppm) as the temperature is reduced below ~80 K, although it never becomes as narrow as it is at high temperature (similar behavior for methyl groups has been observed before in the cryogenic regime[32]). The peak of the aromatic site **b**, which is on the hydrophilic side of the molecule, also remains relatively sharp (LW at half height ≈ 2.4 ppm) at low temperature. The cryogenic behavior of the hydrophilic ^{13}C sites is therefore consistent with a model in which a narrow range of local conformations, or a single local conformation, is populated at low temperature.

The behavior of the ^{13}C resonances associated with the *hydrophobic* structural region is different. All four resonances **h**, **l**, **m**, and **n** of the isobutyl group are strongly broadened by intermediate time scale conformational exchange at temperatures around ~100 K. In addition to the effect of this motion, the ^{13}C peaks of the methyl sites **m** and **n** are also broadened

dx.doi.org/10.1021/jz4026276 | J. Phys. Chem. Lett. 2014, 5, 512−516

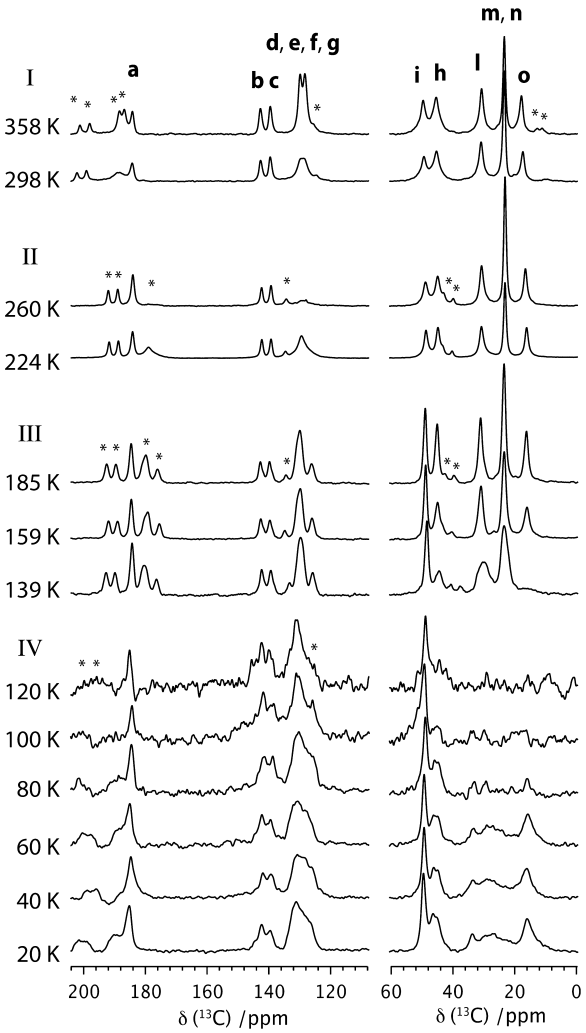

Figure 2. Selection of ^{13}C-CP-MAS spectra of IBU-S acquired in the temperature range from 358 to 20 K. Spinning side bands are marked by asterisks. An unmodulated proton decoupling field was used in all cases, for simplicity. The four series of spectra (I, II, III, IV) were recorded on different apparatus. The magnetic field B_0, rotor diameter d_r, and magic angle spinning frequency ν_r are as follows: Series I: B_0= 9.4 T, d_r = 7.5 mm, $\nu_r \approx$ 6.0 kHz; series II: B_0 = 9.4 T, d_r = 7.5 mm, $\nu_r \approx$ 5.0 kHz; series III: B_0 = 9.4 T, d_r = 4.0 mm, $\nu_r \approx$ 5.0 kHz; series IV: B_0 = 14.1 T, d_r = 2.0 mm, $\nu_r \approx$ 9.0 kHz. Sample masses are 240 (I, II), 150 (III), and 1.5 mg(IV). Experimental details and additional spectra are reported in the SI.

by the intermediate-regime rotation of the methyl groups about their ternary axes. When the sample is cooled further, the peaks do not become narrow. Instead, the relevant spectral regions display a complex and broad inhomogeneous line shape (see the spectrum at 20 K in Figure 2 and Table 1). This is consistent with the freezing in of a wide range of conformations for the hydrophobic sites at cryogenic temperatures. A similar inhomogeneous broadening, although with a narrower chemical shift range, is displayed for the aromatic site **c**, which is closest to the hydrophobic isobutyl group.

To obtain a preliminary interpretation of the frozen conformational distribution for the isobutyl group at cryogenic temperature, we performed a set of density functional theory (DFT) chemical shift calculations for the ^{13}C sites **c**, **h**, **l**, **m**, and **n** over a range of conformations defined by the dihedral angles ϕ_1 and ϕ_2, shown in Figure 1. A B3LYP functional[33,34]

Table 1. Experimental (at 20 K) and Calculated Chemical Shift Distributions for ^{13}C Sites Belonging to the Isobutyl Group (h, l, m, n) and Carbon c (directly bonded to the isobutyl group)

	isotropic chemical shift distributions	
^{13}C site	experimental[a] (20 K)	calculated[b] ($E - E_{min} \leq 0.84$ kJ mol^{-1})
c	141 ± 3 ppm	143 ± 2 ppm
h	46 ± 3 ppm	44 ± 3 ppm
l	28 ± 6 ppm	32 ± 4 ppm
m		23 ± 3 ppm
n		22 ± 3 ppm

[a]The experimental data are taken from the spectrum at 20 K and are reported as the central value of the observed shift distribution ± half of the LW. [b]The calculated data are reported as the average value ± one standard deviation, obtained by taking into account only those conformations that have an energy less than 0.84 kJ mol^{-1} above E_{min}.

and a 6-311+G(d,p) basis set were used in Gaussian09[35] for all NMR calculations. The calculations used the X-ray crystal structure,[30] optimizing at B3LYP/6-31G the hydrogen atom positions and the isobutyl group, which was indeed found to be "disordered" by X-ray diffraction. A model cluster consisting of two adjacent molecules interacting through the sodium carboxylate moiety was used. The longer-range intermolecular interactions were found to be negligible in a sample calculation run on a larger cluster. The molecular energies and the isotropic chemical shifts of the ^{13}C sites **c**, **h**, **l**, **m**, and **n** were estimated for a two-dimensional matrix of dihedral angles (ϕ_1,ϕ_2) (see the SI).

In order to interpret these calculations, we postulated that there is a threshold temperature T_{thresh} below which the kinetics are too slow to allow rapid conformational exchange. The thermally populated conformational distribution existing at temperatures $T > T_{thresh}$ is therefore frozen in when the temperature is cooled below T_{thresh}. The inhomogeneous broadening obtained at very low temperature therefore reflects the thermal distribution of exchanging conformations at the threshold temperature T_{thresh}. The distribution of frozen conformations may be predicted qualitatively by including conformations with energies $E \leq E_{thresh}$, where $E_{thresh} = (E_{min} + k_B T_{thresh})$, k_B is the Boltzmann constant, and E_{min} is the lowest energy of all conformations.

This very rough model allows a qualitative interpretation of the observed results. By selecting $k_B T_{thresh}$ = 0.84 kJ mol^{-1}, which corresponds to T_{thresh} > 100 K, we obtain a set of conformations associated with the isotropic distributions for the ^{13}C sites **c**, **h**, **l**, and **m** shown in Table 1. These distributions are roughly consistent with the 20 K experimental spectrum, if we take into account the strong overlap of the inhomogeneously broadened signals from sites **l**, **m**, and **n**. In addition, we must consider that the signal of methyl carbons **m** and **n** are also broadened by the freezing of the methyl rotation, as in the case of methyl **o**.

This suggests the following model: at temperatures warmer than 100 K, the hydrophobic isobutyl group explores a range of conformations of similar energy. At high temperature, the rate of conformational exchange is fast enough to subject the NMR interactions to motional narrowing. On average, all molecules rapidly explore the complete set of accessible conformations on the NMR time scale; therefore, the peaks are narrow. When the sample is cooled to around ∼100 to ∼130 K, the conformational exchange slows down. The NMR resonances broaden

dx.doi.org/10.1021/jz4026276 | J. Phys. Chem. Lett. 2014, 5, 512−516

due to intermediate time scale exchange between conformations with different isotropic chemical shifts and interference between the exchange process and either the proton decoupling field or the MAS frequency.

At temperatures lower than ∼100 K, the exchange between conformations becomes too slow to allow full thermal equilibration of the sample. The isobutyl group freezes into different metastable conformations that represent local energy minima close to the full range of thermally accessible conformations at ∼100 K. The result is strong inhomogeneous broadening of the corresponding NMR signals. In other words, the isobutyl group experiences a dynamic disorder at high temperatures due to fast interconformational motions and a static disorder at low temperatures due to the distribution of frozen conformations.

It is possible to probe conformational distributions in more detail by using techniques such as two-dimensional correlation spectroscopy.[36] Such methods have been used to investigate solid-state conformational distributions at higher temperature[36−38] but are beyond the scope of this Letter.

In conclusion, the hydrophobic and hydrophilic regions of IBU-S display contrasting behavior in the context of cryogenic MAS NMR. The hydrophilic region remains well-structured at cryogenic temperatures and consistently displays narrow peaks, except for the associated methyl group, whose peak broadens due to hindered three-fold rotation at around ∼100 K but that narrows again at lower temperatures. The hydrophobic region, with its flexible isobutyl group, on the other hand, displays the NMR signature of a broad frozen conformational distribution at very low temperature. This study shows the range of phenomena that may be displayed, even by small molecules, in cryogenic solid-state NMR.

■ ASSOCIATED CONTENT

Supporting Information

XRPD data, solid-state NMR experimental details and additional spectra, and complete results of DFT calculations. This material is available free of charge via the Internet at http://pubs.acs.org.

■ AUTHOR INFORMATION

Corresponding Author

*E-mail: mhl@soton.ac.uk.

Notes

The authors declare no competing financial interest.

■ ACKNOWLEDGMENTS

We thank EPSRC (U.K.) and ERC for funds and Salvatore Mamone for help. We thank Prof. Paola Paoli, Dr. Patrizia Rossi, and Dr. Eleonora Macedi (University of Florence) for providing the XRPD data.

■ REFERENCES

(1) Samoson, A.; Tuherm, T.; Past, J.; Reinhold, A. New Horizons for Magic-Angle Spinning NMR. *Top. Curr. Chem* **2005**, *246*, 15−31.
(2) Sarkar, R.; Concistrè, M.; Johannessen, O. G.; Beckett, P.; Denning, M.; Carravetta, M.; Al-Mosawi, M.; Beduz, C.; Yang, Y.; Levitt, M. H. An NMR Thermometer for Cryogenic Magic-Angle Spinning NMR: The Spin-Lattice Relaxation of ^{127}I in Cesium Iodide. *J. Magn. Reson.* **2011**, *212*, 460−463.
(3) Concistrè, M.; Johannessen, O. G.; Carignani, E.; Geppi, M.; Levitt, M. H. Magic-Angle Spinning NMR of Cold Samples. *Acc. Chem. Res.* **2013**, *46*, 1914−1922.
(4) Tycko, R. NMR at Low and Ultralow Temperatures. *Acc. Chem. Res.* **2013**, *46*, 1923−1932.
(5) Hackmann, A.; Seidel, H.; Kendrick, R.; Myhre, P.; Yannoni, C. Magic-Angle Spinning NMR at Near-Liquid-Helium Temperatures. *J. Magn. Reson.* **1988**, *79*, 148−153.
(6) Matsuki, Y.; Ueda, K.; Idehara, T.; Ikeda, R.; Ogawa, I.; Nakamura, S.; Toda, M.; Anai, T.; Fujiwara, T. Helium-Cooling and -Spinning Dynamic Nuclear Polarization for Sensitivity-Enhanced Solid-State NMR at 14 T and 30 K. *J. Magn. Reson.* **2012**, *225*, 1−9.
(7) Thurber, K. R.; Tycko, R. Biomolecular Solid State NMR with Magic-Angle Spinning at 25K. *J. Magn. Reson.* **2008**, *195*, 179−186.
(8) Beckett, P.; Denning, M. S.; Heinmaa, I.; Dimri, M. C.; Young, E. A.; Stern, R.; Carravetta, M. High Resolution ^{11}B NMR of Magnesium Diboride Using Cryogenic Magic Angle Spinning. *J. Chem. Phys.* **2012**, *137*, 114201.
(9) Beduz, C.; Carravetta, M.; Chen, J. Y.-C.; Concistrè, M.; Denning, M.; Frunzi, M.; Horsewill, A. J.; Johannessen, O. G.; Lawler, R.; Lei, X.; Levitt, M. H.; Li, Y.; Mamone, S.; Murata, Y.; Nagel, U.; Nishida, T.; Ollivier, J.; Rols, S.; Rõõm, T.; Sarkar, R.; Turro, N. J.; Yang, Y. Quantum Rotation of ortho and para-Water Encapsulated in a Fullerene Cage. *Proc. Natl. Acad. Sci. U.S.A.* **2012**, *109*, 12894−12898.
(10) Lipton, A. S.; Heck, R. W.; de Jong, W. A.; Gao, A. R.; Wu, X.; Roehrich, A.; Harbison, G. S.; Ellis, P. D. Low Temperature ^{65}Cu NMR Spectroscopy of the Cu^{+} Site in Azurin. *J. Am. Chem. Soc.* **2009**, *131*, 13992−13999.
(11) Concistrè, M.; Gansmüller, A.; McLean, N.; Johannessen, O. G.; Marín Montesinos, I.; Bovee-Geurts, P. H. M.; Verdegem, P.; Lugtenburg, J.; Brown, R. C. D.; DeGrip, W. J.; et al. Double-Quantum ^{13}C Nuclear Magnetic Resonance of Bathorhodopsin, the First Photointermediate in Mammalian Vision. *J. Am. Chem. Soc.* **2008**, *130*, 10490−10491.
(12) Gansmüller, A.; Concistrè, M.; McLean, N.; Johannessen, O. G.; Marín-Montesinos, I.; Bovee-Geurts, P. H. M.; Verdegem, P.; Lugtenburg, J.; Brown, R. C. D.; Degrip, W. J.; et al. Towards an Interpretation of ^{13}C Chemical Shifts in Bathorhodopsin, a Functional Intermediate of a G-Protein Coupled Receptor. *Biochim. Biophys. Acta* **2009**, *1788*, 1350−1357.
(13) Concistrè, M.; Gansmüller, A.; McLean, N.; Johannessen, O. G.; Marín Montesinos, I.; Bovee-Geurts, P. H. M.; Brown, R. C. D.; DeGrip, W. J.; Levitt, M. H. Light Penetration and Photoisomerization in Rhodopsin Studied by Numerical Simulations and Double-Quantum Solid-State NMR Spectroscopy. *J. Am. Chem. Soc.* **2009**, *131*, 6133−6140.
(14) Bajaj, V. S.; Mak-Jurkauskas, M. L.; Belenky, M.; Herzfeld, J.; Griffin, R. G. Functional and Shunt States of Bacteriorhodopsin Resolved by 250 GHz Dynamic Nuclear Polarization-Enhanced Solid-State NMR. *Proc. Natl. Acad. Sci. U.S.A.* **2009**, *106*, 9244−9249.
(15) Barnes, A. B.; Corzilius, B.; Mak-Jurkauskas, M. L.; Andreas, L. B.; Bajaj, V. S.; Matsuki, Y.; Belenky, M. L.; Lugtenburg, J.; Sirigiri, J. R.; Temkin, R. J.; et al. Resolution and Polarization Distribution in Cryogenic DNP/MAS Experiments. *Phys. Chem. Chem. Phys.* **2010**, *12*, 5861−5867.
(16) Debelouchina, G. T.; Bayro, M. J.; van der Wel, P. C. A.; Caporini, M. A.; Barnes, A. B.; Rosay, M.; Maas, W. E.; Griffin, R. G. Dynamic Nuclear Polarization-Enhanced Solid-State NMR Spectroscopy of GNNQQNY Nanocrystals and Amyloid Fibrils. *Phys. Chem. Chem. Phys.* **2010**, *12*, 5911−5919.
(17) Bayro, M. J.; Debelouchina, G. T.; Eddy, M. T.; Birkett, N. R.; MacPhee, C. E.; Rosay, M.; Maas, W. E.; Dobson, C. M.; Griffin, R. G. Intermolecular Structure Determination of Amyloid Fibrils with Magic-Angle Spinning and Dynamic Nuclear Polarization NMR. *J. Am. Chem. Soc.* **2011**, *133*, 13967−13974.
(18) Linden, A. H.; Lange, S.; Franks, W. T.; Akbey, U.; Specker, E.; van Rossum, B.-J.; Oschkinat, H. Neurotoxin II Bound to Acetylcholine Receptors in Native Membranes Studied by Dynamic Nuclear Polarization NMR. *J. Am. Chem. Soc.* **2011**, *133*, 19266−19269.
(19) Akbey, Ü.; Linden, A. H.; Oschkinat, H. High-Temperature Dynamic Nuclear Polarization Enhanced Magic-Angle-Spinning NMR. *Appl. Magn. Reson.* **2012**, *43*, 81−90.

(20) Gelis, I.; Vitzthum, V.; Dhimole, N.; Caporini, M. A.; Schedlbauer, A.; Carnevale, D.; Connell, S. R.; Fucini, P.; Bodenhausen, G. Solid-State NMR Enhanced by Dynamic Nuclear Polarization as a Novel Tool for Ribosome Structural Biology. *J. Biomol. NMR* **2013**, *56*, 85−93.
(21) Thurber, K. R.; Potapov, A.; Yau, W.-M.; Tycko, R. Solid State Nuclear Magnetic Resonance with Magic-Angle Spinning and Dynamic Nuclear Polarization Below 25 K. *J. Magn. Reson.* **2013**, *226*, 100−106.
(22) Bajaj, V. S.; van der Wel, P. C. A; Griffin, R. G. Observation of a Low-Temperature, Dynamically Driven Structural Transition in a Polypeptide by Solid-State NMR Spectroscopy. *J. Am. Chem. Soc.* **2009**, *131*, 118−128.
(23) Long, J. R.; Sun, B. Q.; Bowen, A.; Griffin, R. G. Molecular Dynamics and Magic Angle Spinning NMR. *J. Am. Chem. Soc.* **1994**, *116*, 11950−11956.
(24) Hodgkinson, P. Intramolecular Motion in Crystalline Organic Solids. *Encycl. Nucl. Magn. Reson.* **2009**, 46−82.
(25) Rothwell, W. P.; Waugh, J. S. Transverse Relaxation of Dipolar Coupled Spin System under rf Irradiation: Detecting Motions in Solid. *J. Chem. Phys.* **1981**, *74*, 2721−2732.
(26) Duer, M. J. Solid-State NMR Studies of Molecular Motion. *Annu. Rep. NMR Spectrosc.* **2001**, *43*, 1−58.
(27) Apperley, D. C.; Harris, R. K.; Hodgkinson, P. *Solid-State NMR Basic Principles and Practice*; Momentum Press: New York, 2012.
(28) Apperley, D. C.; Markwell, A. F.; Frantsuzov, I.; Ilott, A. J.; Harris, R. K.; Hodgkinson, P. NMR Characterisation of Dynamics in Solvates and Desolvates of Formoterol Fumarate. *Phys. Chem. Chem. Phys.* **2013**, *15*, 6422−6430.
(29) Carignani, E.; Borsacchi, S.; Geppi, M. Dynamics by Solid-State NMR: Detailed Study of Ibuprofen Na Salt and Comparison with acidic Ibuprofen. *J. Phys. Chem. A* **2011**, *115*, 8783−8790.
(30) Zhang, Y.; Grant, D. J. W. Similarity in Structures of Racemic and Enantiomeric Ibuprofen Sodium Dihydrates. *Acta Crystallogr., Sect. C* **2005**, *61*, m435−438.
(31) Geppi, M.; Guccione, S.; Mollica, G.; Pignatello, R.; Veracini, C. A. Molecular Properties of Ibuprofen and Its Solid Dispersions with Eudragit RL100 Studied by Solid-State Nuclear Magnetic Resonance. *Pharm. Res.* **2005**, *22*, 1544−1555.
(32) Macho, V.; Kendrick, R.; Yannoni, C. S. Cross Polarization Magic-Angle Spinning NMR at Cryogenic Temperatures. *J. Magn. Reson.* **1983**, *52*, 450−456.
(33) Becke, A. D. Density-Functional Exchange-Energy Approximation with Correct Asymptotic Behavior. *Phys. Rev. A* **1988**, *38*, 3098−3100.
(34) Lee, C.; Yang, W.; Parr, R. G. Development of the Colle−Salvetti Correlation-Energy Formula into a Functional of the Electron Density. *Phys. Rev. B* **1988**, *37*, 785−789.
(35) Frisch, M. J.; Trucks, G. W.; Schlegel, H. B.; Scuseria, G. E.; Robb, M. A.; Cheeseman, J. R.; Scalmani, G.; Barone, V.; Mennucci, B.; Petersson, G. A.; et al. *Gaussian 09*, revision D.01; Gaussian Inc.: Wallingford, CT, 2009.
(36) Cadars, S.; Lesage, A.; Pickard, C. J.; Sautet, P.; Emsley, L. Characterizing Slight Structural Disorder in Solids by Combined Solid-State NMR and First Principles Calculations. *J. Phys. Chem. A* **2009**, *113*, 902−911.
(37) Heise, H.; Luca, S.; de Groot, B. L.; Grubmüller, H.; Baldus, M. Probing Conformational Disorder in Neurotensin by Two-Dimensional Solid-State NMR and Comparison to Molecular Dynamics Simulations. *Biophys. J.* **2005**, *89*, 2113−2120.
(38) Hu, K.-N.; Havlin, R. H.; Yau, W.-M.; Tycko, R. Quantitative Determination of Site-Specific Conformational Distributions in an Unfolded Protein by Solid-State Nuclear Magnetic Resonance. *J. Mol. Biol.* **2009**, *392*, 1055−1073.